The Pharmaceutical and Chemical Journal, 2018, 5(5):23-34

Available online www.tpcj.org

Research Article

ISSN: 2349-7092
CODEN(USA): PCJHBA

Growth, Vibrational and Antimicrobial Activity Studies on Glycinium Dihydrogen Phosphate Complex Crystal

Muthuselvi C.[1]*, Uma Maheswari P.[2], Ravikumar B.[1]

[1]Department of Physics, Devanga Arts College, Aruppukottai- 626 101, Tamilnadu, India
[2]Department of Physics, Madurai Kamaraj University Evening College, Madurai- 625002, Tamilnadu, India

Abstract The single crystal of glycinium dihydrogen phosphate was grown at room temperature by the slow evaporation method. The well grown transparent crystal was subjected to the single crystal XRD study for confirmation. The powder XRD study shows crystalline nature and purity of the title crystal. The vibrational analysis of title crystal was accomplished through the FT-IR and FT-Raman spectroscopy techniques. The optical property and energy gap was analyzed by the UV-Visible spectroscopy study. The surface morphology and elemental analysis were done with the help of SEM with EDX analyzes. The antimicrobial activity of title crystal was tested against the four different micro-organisms by disc diffusion method.

Keyword: glycinium dihydrogen phosphate, XRD, antimicrobial activity, FT-IR, FT-Raman, SEM, EDX.

1. Introduction

Glycine is the simplest and sweet-tasting non-essential amino acid which is necessary ones for a healthy digestive system [1]. It is found in various high-protein foods like beans, fish, meat, milk, and cheese [2]. It is known as an anti-aging amino acid which is used to prevent the cellular damage and various signs of aging [3]. According to some researches on glycine showed that it can also inhibit some types of cancer through antioxidants [4, 5]. It has three different polymorphismsie.,α-glycine, β-glycine and γ–glycine [6-8]. Many researchers to grow glycine single crystal with different combination of inorganic salts such as phosphoric acid [9], hydrofluoric acid [10], hydro bromic acid [11], nitric acid [12] and hydro chloric acid [13]. Also, the structural studies of amino acid complexes were reported by many authors in the past few years [14, 15]. Glycine is known to react with the ortho phosphoric acid leading to the formation of glycinium dihydrogen phosphate and the crystal structure was already reported by Averbuch-Pouchot et al. [16] .In the present work, single crystal XRD and powder XRD, FT-IR, FT-Raman, UV-Visible spectroscopy, SEM with EDAX studies were carried out. Apart from these, the antibacterial activity study seems to be enhanced because none of them were reported to this property for this compound.

2. Materials and Method

Materials

Commercially available raw materials of analar grade of glycine and ortho phosphoric acid were purchased from the local scientific company, Madurai, India.

Slow evaporation Method

The equimolar ratio (2: 1) of glycine and ortho phosphoric acid were dissolved in distilled water and it was stirred for 1 hour. Then it was filtered using high quality filter paper. The filtered solution was poured into the petri dish.

Now the petri dish was tightly closed with thick filter paper due to minimize rate of evaporation at room temperature. After a period of 10 days bulk transparent crystals of glycinium dihydrogen phosphate were harvested. The photographic view of grown crystal is depicted in figure 1.

Figure 1: Grown crystal of glycinium dihydrogen phosphate

3. Characterization Techniques

A good quality grown crystal of glycinium dihydrogen phosphate was confirmed by single crystal X-ray diffraction analysis using Bruker SMART APEX CCD diffractometer with Mo Kα radiation (λ = 0.71073 Å) . The XPERT−PRO X–ray diffractometer with Cu Kα (λ = 1.54060 Å) radiation was used to record the powder diffraction pattern. The FT−IR vibrational spectrum was recorded by using SHIMADZU FT−IR spectrometer in the range 4000-400 cm^{-1}. Also, the FT−Raman spectrum was recorded by using the BRUKER: RFS 27 Raman spectrometer in the wavenumber range 4000-400 cm^{-1}. The optical absorption spectrum has been recorded with SHIMADZU−UV1800 double beam spectrometer in the wavelength range 200−1100 nm insteps of 1 nm. The surface morphology and elemental analysis has been carried out by CARLZEISS EVO18 scanning electron microscope. The antimicrobial activity of parent and its complex crystals were tested against four different kinds of micro-organisms by disc diffusion method.

4. Results and Discussion

4.1. Single crystal XRD

The unit cell parameter of the title compound was determined using the Bruker SMART APEX CCD single crystal X-ray diffractometer. This result showed that cell parameter values of the grown crystal are exactly matched with already reported values [16]. The experimentally obtained cell parameter values of title crystal are tabulated in Table 1.

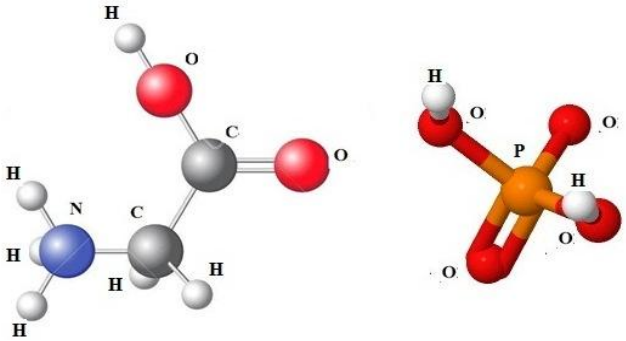

Figure 2: Molecular structure of glycinium dihydrogen phosphate crystal

The single crystal XRD study reveals that the grown crystal is a complex one, since the one proton of phosphoric acid is liberated and protonated with glycine NH_2 group, leading to formation of glyciniumcation and dihydrogen phosphate anion. Here, the carboxylic group of glycine is not deprotonated and so its configuration became as

$HOOC\text{-}CH_2\text{-}NH_3^+$. Also this study confirms the grown crystal crystallizes in the monoclinic system with space group $P2_1/c$. The molecular structure of glycinium dihydrogen phosphate crystal is shown in figure 2.

Table 1: Crystallographic data of glycinium dihydrogen phosphate crystal

Lattice Parameters	Present Study	Already reported [16]
Compound name	Glycinium dihydrogen phosphate	Glycinium dihydrogen phosphate
Empirical formula	$C_2H_6NO_2^+H_2PO_4^-$	$C_2H_6NO_2^+H_2PO_4^-$
Molecular formula weight	173.06	173.06
Unit cell Dimensions	a = 9.575 (3) (Å)	a = 9.580 (2) (Å)
	b = 7.838(3) (Å)	b = 7.840 (2) (Å)
	c = 9.248 (5) (Å)	c = 9.249 (3) (Å)
	$\alpha = 90^\circ$	$\alpha = 90^\circ$
	$\beta = 114.5\ (4)^\circ$	$\beta = 114.7\ (2)^\circ$
	$\gamma = 90^\circ$	$\gamma = 90^\circ$
Volume	625 $(Å)^3$	631 $(Å)^3$
Crystal system	Monoclinic	Monoclinic
Space group	$P2_1/c$	$P2_1/c$

4.2. Powder XRD Analysis

The powder XRD pattern of glycinium dihydrogen phosphate crystal is shown in figure 3. The appearance of sharp and strong peaks confirmed the good crystallinity and purity of the grown crystal. The characteristic peak of this compound has seemed at around 29.80°. The INDX software was used to index the PXRD patterns. The average crystalline size of title crystal was determined by using the Debye-Scherrer equation, which can be written as,

$$D = \frac{K\lambda}{\beta \cos\theta}$$

where,

D = average crystallite size

K= dimensionless shape factor (0.94)

λ = wavelength of X-ray radiation (Cu Kα = 1.54060 Å)

θ = diffraction angle

β= Full width at half maximum intensity

The Dislocation density can be calculated from,

$$\delta = \frac{1}{D^2}\ m^2$$

where,

δ is dislocation density,

D is the crystallite size

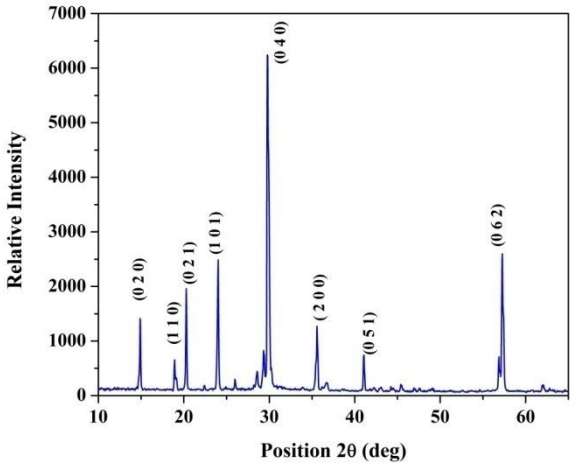

Figure 3: Diffraction patterns for glycinium dihydrogen phosphate crystal

For glycinium dihydrogen phosphate crystal, the average crystalline size was found to be as 27 nm. Also, the dislocation density was determined as 1.37 $X10^{15}m^2$.

4.3. Vibrational analysis

The glycinium dihydrogen phosphate crystal has $[NH_3]^+$, CH_2, COOH and $[H_2PO_4]^-$functional groups. The FT-IR and FT-Raman spectra of title compound are shown in figure 4 and figure 5 respectively. The detailed wavenumber assignments for the glycinium dihydrogen phosphate crystal are presented in Table 2.

Vibrations of –[NH$_3$]$^+$cation

Normally the antisymmetric and symmetric stretching modes of – $[NH_3]^+$ group were found in the region of 3200 cm^{-1} and 2800 cm^{-1} [17]. In the present study, ν_{as}–$[NH_3]^+$ mode is identified as a strong broad band at 3171cm^{-1} in IR and as a weak band at 3140 cm^{-1} in Raman spectra for this mode. Also ν_s–$[NH_3]^+$ mode is attributed at 2965 cm^{-1}, 2889 cm^{-1}, 2825 cm^{-1} in IR and at 2970 cm^{-1}, 2887 cm^{-1}, 2821 cm^{-1} in Raman spectra. The antisymmetric and symmetric bending wavenumbers for–$[NH_3]^+$ group were normally expected to fall in the region of 1625-1550 cm^{-1} and 1550-1505 cm^{-1} respectively [17, 18]. For the title crystal, δ_{as}–$[NH_3]^+$ mode is assigned at 1611 cm^{-1} in IR spectrum and the δ_s–$[NH_3]^+$ band is attributed at 1554 cm^{-1}, 1506 cm^{-1} in IR and at 1568 cm^{-1}, 1511 cm^{-1} in Raman spectra. The experimentally observed stretching and bending modes of –$[NH_3]^+$ group for the title compound are deviated from the free ion due to the presence of hydrogen bonding network.

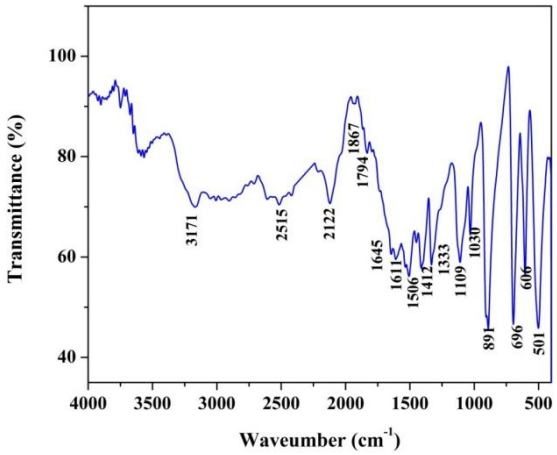

Figure 4: FT-IR spectrum of glycinium dihydrogen phosphate crystal

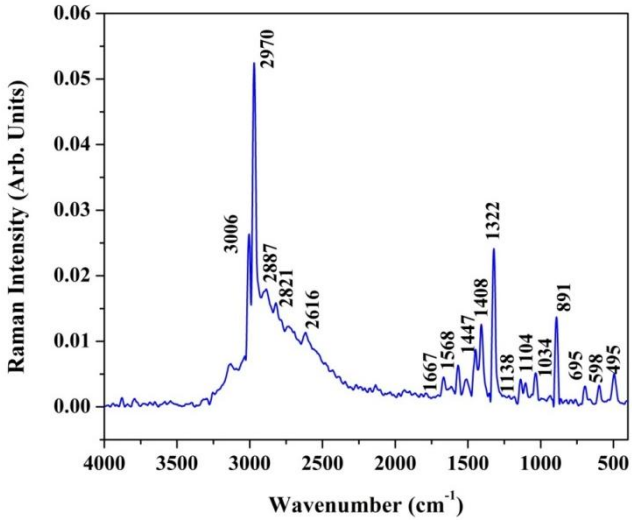

Figure 5: FT-Raman spectrum of glycinium dihydrogen phosphate crystal

Table 2: Wavenumber assignments for glycinium dihydrogen phosphate crystal in FT – IR and FT – Raman spectra

FT – IR ($\bar{\upsilon}$ / cm^{-1})	**FT− Raman ($\bar{\upsilon}$ / cm^{-1})**	**Assignment**
3171 (s, br)	3140 (w)	$\nu_{as}[NH_3]^+$
3000 (sh)	3006 (m)	ν (O-H)
2965 (w)	2970(s)	$\nu_s[NH_3]^+$; ν_{as} (CH_2)
2889 (w)	2887(m)	$\nu_s[NH_3]^+$; ν_s (CH_2)
2825 (w)	2821 (m)	$\nu_s[NH_3]^+$
1794 (w)	-	ν_{as} (C=O)
1734(m)	-	ν_{as}(C=O)
1645(w)	1667 (w)	ν_s (C=O)
1611(m)	-	$\delta_{as}[NH_3]^+$
1554(sh)	1568(m)	$\delta_s[NH_3]^+$
1506(m)	1511(w)	$\delta_s[NH_3]^+$
1451 (w)	1447(m)	ρ (CH_2); β(O-H)
1412(m)	1408(m)	β(O-H)
1333(s)	1322(s)	ω(CH_2)
1239(w)	1244 (w)	ν (C-O); t(CH_2); β(P-OH)
1191(sh)	-	ν (P=O)
1134 (sh)	1138 (w)	ν (C-N); ν_{as} $[H_2PO_4]^-$
1109 (m)	1109 (w)	ν (C-N); ν (C-C)
1064(sh)	-	ν_{as} $[H_2PO_4]^-$
1030(m)	1034 (w)	ν (C-N); ν (C-C)
976(sh)	-	ν_{as} $[H_2PO_4]^-$
891(s)	891(m)	γ(O-H); ν_s $[H_2PO_4]^-$; ν(P-OH)
839(sh)	861(w)	γ(P-OH); ν (C-C)
606 (w)	-	δ_{as} $[H_2PO_4]^-$
501(w)	-	δ_{as} $[H_2PO_4]^-$
417 (sh)	-	δ_{as} $[H_2PO_4]^-$
-	359(w)	δ_s $[H_2PO_4]^-$
-	342(w)	δ_s $[H_2PO_4]^-$

w–weak; s– strong; m– medium; sh- shoulder; υ– stretching; υ_s– symmetric stretching;υ_{as}–anti symmetric stretching; δ_s- symmetric bending; δ_{as}- antisymmetric bending; γ– out–of–plane bending; β– in–plane bending; ρ- rocking; t-twisting; ω-wagging

Vibrationsof $[H_2PO_4]^-$ anion

In the free state, the phosphate ion exist in T_d symmetry which has symmetric stretching $\nu_1(A_1)$, antisymmetric stretching $\nu_3(F_2)$, symmetric bending $\nu_2(E)$ and antisymmetric bending $\nu_4(F_2)$ internal vibrational modes. These wavenumbers occur at 936 cm^{-1} (ν_{sym}), 420 cm^{-1} (δ_{sym}), 1004 cm^{-1} (ν_{asym}) and 573 cm^{-1} (δ_{asym})[19, 20]. But, the molecular symmetry of $[H_2PO_4]^-$ion reduces to C_{2v} symmetry owing to the presence of two P−OH bonds. As a result, ν_2 splits into two components (A1 + A2) and ν_3 and ν_4 split into three components (A1 + B1 + B2) each [19]. The symmetric stretching mode (A_1) normally occurs at 880 cm^{-1} and the symmetric bending mode E splits into two, appearing at 385 (A_1) and 373 (A_2) cm^{-1}. The antisymmetric stretching mode (F_2) splits into three occurring at 1090 (A_1), 1123 (B_1) and 940 (B_2) cm^{-1}. The antisymmetric bending mode (F_2) has also lost its degeneracy and was expected to occur at 525 (A_1), 510 (B_1) and 503 (B_2) cm^{-1}. All the species were both infrared and Raman active except for A_2 species, which was only Raman active [21]. In the present study, ν_{as} $[H_2PO_4]^-$ mode is identified at 1064(A_1), 1134(B_1), 976 (B_2) cm^{-1}in IR and the symmetric stretching mode is observed in IR and

Raman spectra at 891(A_1), 891(A_1) cm^{-1} respectively. Also, the symmetric bending mode of this group is attributed at 359, 342 cm^{-1} in Raman spectrum only and antisymmetric bending mode is identified at 606(A_1), 417(B_1) and 501 (B_2) cm^{-1} in IR spectrum only. All these assignments confirm the existence of dihydrogen phosphate anion in the C_{2v} symmetry and it is clearly identified from the Table 3.The P–OH group has a strong band in the region 1040 – 810 cm^{-1} which is due to the stretching of P–OH bands [21]. The medium bands occur at 891cm^{-1}in IR and at 891 cm^{-1} in Raman spectra are assigned to P–OH stretching vibration of title crystal. The in-plane and out-of-plane bending vibrations of P–OH group occur in the region1350–1200 $cm^{-1}$and 950–750 cm^{-1} respectively [22].

Table 3: Vibrational distribution of $[PO_4]^{3-}$ ion to $[H_2PO_4]^-$ ion

T_d $[PO_4]^{3-}$(cm^{-1})	C_{2v} $[H_2PO_4]^-$(cm^{-1})	Present Study (cm^{-1})
A_1 (936)	A_1 (887)	A_1 (891)
E (420)	A_1 (357)	A_1 (359)
	A_2 (338)	A_2 (342)
F_2 (1004)	A_1 (1096)	A_1 (1064)
	B_1 (1132)	B_1 (1134)
	B_2 (964)	B_2 (976)
F_2(573)	A_1 (529)	A_1 (606)
	B_1 (453)	B_1 (417)
	B_2 (500)	B_2 (501)

For the title compound these modes are identified in IR spectrum at 1239 cm^{-1}, 839 cm^{-1} and in Raman spectrum at 1244 cm^{-1}, 861 cm^{-1} respectively. The stretching vibrations of P=O generally give rise to strong band in the region 1300 – 1140 cm^{-1} for dihydrogen phosphate. The absorption bands at 1191 cm^{-1} in IR spectrum is assigned to P=O stretching mode of glycinium dihydrogen phosphate crystal.

CH_2 group vibrations

The regions between 3000–2900 cm^{-1} and 2900 and 2800 cm^{-1} were identified as antisymmetric and symmetric stretching vibrations of CH_2 group respectively [23- 25]. The CH_2 symmetric stretching vibration for 6′-(3-Bromo phenyl)-7′-nitro-1′,6′,7′,7a′-tetrahydro-3′H-spiro[indeno[1,2-b]quinoxaline-11,5′-pyrrolo[1,2-c]thiazole] molecule at 2929 cm^{-1} in IR and at 2942 cm^{-1} in Raman spectra for antisymmetric stretching mode of CH_2 group were reported by Muthuselvi et al. [26]. Also, the symmetric stretching mode of the CH_2 group was assigned at 2871, 2867 cm^{-1} in both spectra. In the present work, bands are recognized at 2965 cm^{-1}, 2889 $cm^{-1}$and at 2970 cm^{-1}, 2887 cm^{-1} in both spectra is assigned to $\upsilon_{as}(CH_2)$and $\upsilon_s(CH_2)$ modes respectively. The CH_2bending mode wavenumber assignment orders were specified as follows: CH_2scis> CH_2wag > CH_2 twist > CH_2 rock [27]. The CH_2 scissoring, wagging and twisting modes fall in the range 1482–1437 cm^{-1}, 1390–1180 cm^{-1} and 730 cm^{-1}- 720 cm^{-1} respectively [26, 27]. In the present study, the absorption bands at 1451 cm^{-1} in IR and at 1447 cm^{-1} in Raman spectra is assigned to CH_2 scissoring mode. Also, CH_2 wagging and twisting modes are attributed at the 1333 cm^{-1}, 1239 cm^{-1} (IR), 1322 cm^{-1} (Raman). The rocking mode is not identified for title compound. The CH_2 group vibrational wavenumbers is not much shifting which reveals that this group does not make any bonding with other groups.

Vibrations of COOH group

The carboxylic group C=O antisymmetric and symmetric stretching wavenumbers occur in the region of 1720-1680 cm^{-1} and 1680-1640 cm^{-1} respectively [28]. In the present study, the bands arise at 1794, 1734 cm^{-1} in IR is assigned to ν_{as} (C=O) mode and the bands are identified at 1645 cm^{-1} in IR and 1667 cm^{-1} in Raman is consigned to the ν_s(C=O) mode. The ν (C-O) mode normally occurs in the region of 1320–1210 cm^{-1} [29]. The wavenumber at 1239 cm^{-1} in IR spectrum is attributed to ν (C-O) mode. The O–H stretch from CO–OH group was identified at 3065–2826 cm^{-1}[26]. It is ascribed as a weak bands at 3000 $cm^{-1}$and at3006 cm^{-1}in both spectra for title compound. The in-plane and out -of plane bending wavenumbers of O–H group appears in the region between 1440–1395 cm^{-1} and 960–875 cm^{-1}respectively [28, 29]. In the present work, β(O–H) mode is observed at 1451 cm^{-1}, 1412 cm^{-1} in IR and

at 1447 cm^{-1}, 1408cm^{-1} in Raman spectra respectively. Also γ(O–H) mode is attributed at 891 cm^{-1} in both spectra of title compound.

Vibrations of other groups

The stretching and bending modes C-C group normally falls in the range 1117-870 cm^{-1}[30]. The C-N absorption bands for aliphatic amines appear in the region of 1250 – 1020 cm^{-1} [30]. In the present study the bands identified at 1109 cm^{-1}, 1030 cm^{-1}, 839 cm^{-1} in IR spectrum and at 1104 cm^{-1}, 1034 cm^{-1}, 861 cm^{-1} in Raman spectrum is assigned to the ν (C-C) mode of title compound. Also, the ν (C-N) mode is attributed at 1134cm^{-1} and 1138 cm^{-1} in both spectra. The other bands assigned to this mode mixed with C -C stretching vibration.

4.4. Optical analysis

The SHIMADZU−UV1800 double beam spectrometer was used to obtain the absorbance spectrum of title crystal in the wavelength range 200−1100 nm. The experimentally recorded absorbance spectrum is shown in Figure 6. The lower cut-off wavelength was found to be at 240 nm. The title crystal has 100% transmittance in the entire visible region which makes usefulness of this material in optical application. The Tauc's relation $(\alpha h\nu)^2 = A(h\nu - E_g)$ was used to determined energy gap E_g by plotting the $(\alpha h\nu)^2$ Vs photon energy and extrapolate the linear portion of $(\alpha h\nu)^2$ to the photon energy axis gives the energy gap value of title crystal

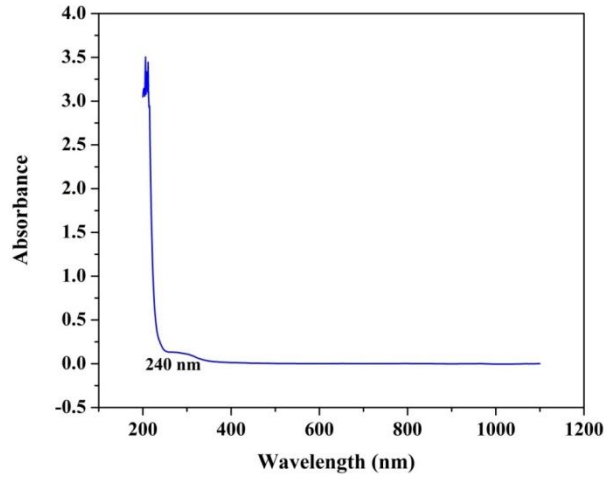

Figure 6: Absorbance spectrum for glycinium dihydrogen phosphate crystal

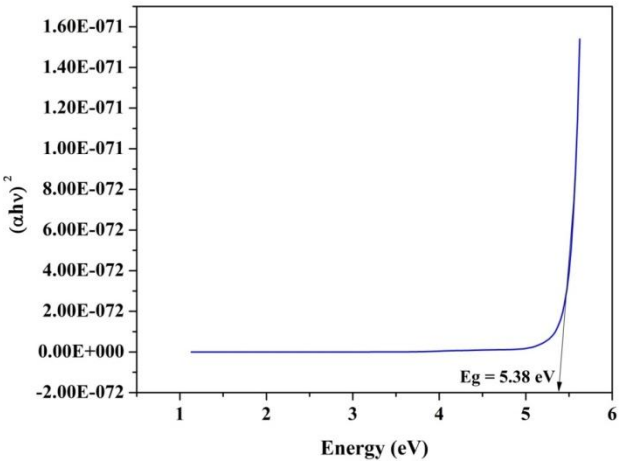

Figure 7: Optical band gap forglycinium dihydrogen phosphate crystal

The energy band gap was found at 5.38 eV from the Figure 7 and this band gap value reveals that the grown crystal is a typical of dielectric material.

4.5. SEM with EDX Analyzes

The SEM with EDX analyzes was used to analyze morphology and elemental composition of the title crystal. The SEM micro photographic images of title crystal with two different magnifications are illustrated in Figure.8. The glycinium dihydrogen phosphate crystal has smooth surface and well defined hexagonal shape morphology. These images revealed that the grown crystal has small voids and porous nature in the surface. However, the major part of the crystal has well defined hexagonal shape.

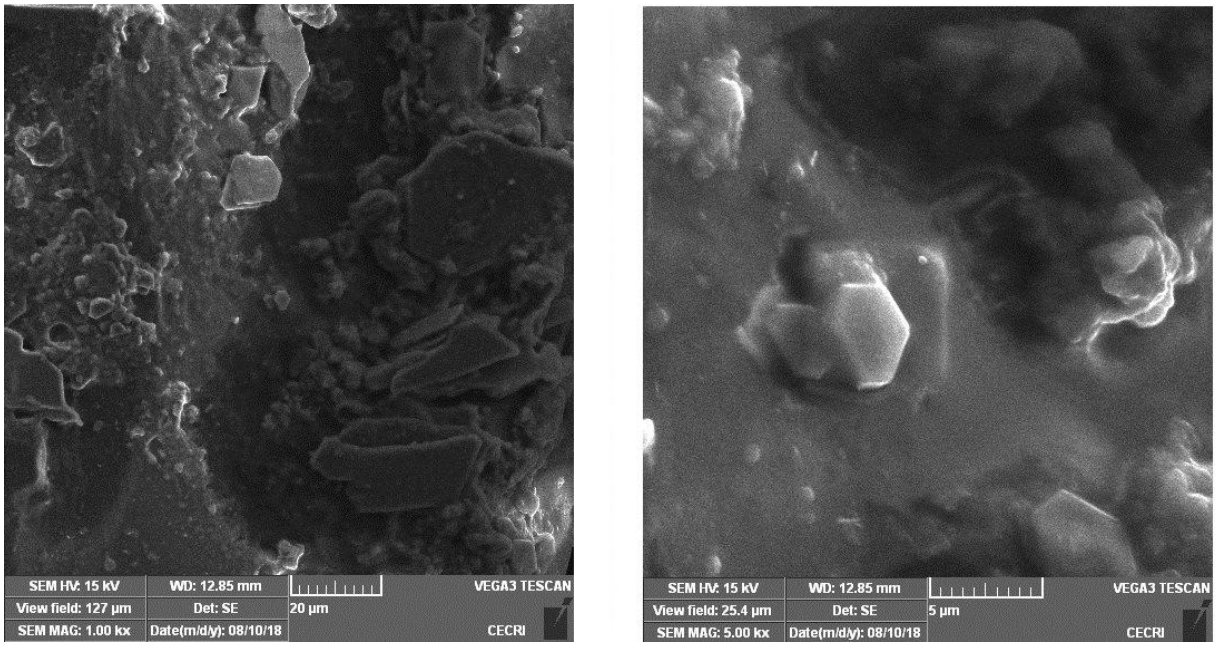

Figure 8: SEM photograph forglycinium dihydrogen phosphate crystal

The EDX spectrum for glycinium dihydrogen phosphate crystal is displayed in Figure.9. The elemental composition present in crystal is shown in Table 3.

Table 3: Elemental composition for glycinium dihydrogen phosphate crystal

Elements	Glycinium dihydrogen phosphate	
	Atomic%	**Weight %**
C	59.42	51.74
O	39.09	45.34

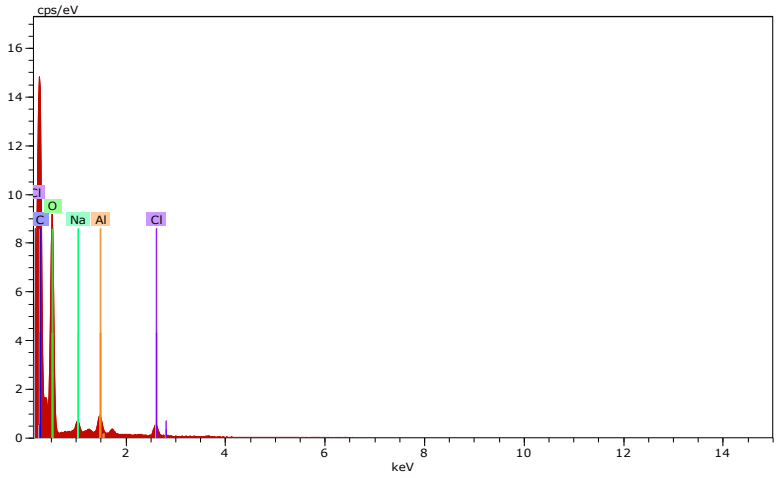

Figure 9: EDX chart for glycinium dihydrogen phosphate crystal

From the EDX spectrum, the presence of C and O elements are confirmed in the glycinium dihydrogen phosphate crystal.

4.6. Antimicrobial activity study

The Bacillus subtilis, Micrococcus, Salmonella typhi and Pseudomonas micro-organisms were tested to analyze the antimicrobial activity of glycine and glycinium dihydrogen phosphatecrystals by disc diffusion method. The photographic view of bacterial screening for parent and its complex crystals with 50µg/ml and 100 µg /l concentrations are shown in figure.10a and 10b respectively. The measured diameter zone of inhibition of these microorganisms is given in Table 4.

Table 4: Effective values of inhibited zone for glycine and glycinium dihydrogen phosphate crystal

S. No.	Micro-organisms	Zone of inhibition for glycine		Zone of inhibition for glycinium dihydrogen phosphate crystal	
		50 µl (mm)	100 µl (mm)	50 µl (mm)	100 µl (mm)
1.	*Bacillus subtilis*	NIL	NIL	NIL	NIL
2.	*Micrococcus*	NIL	4	NIL	NIL
3.	*Salmonella typhi*	NIL	NIL	NIL	NIL
4.	*Pseudomonas*	NIL	NIL	NIL	NIL

*NIL- No antimicrobial activity; mm- Zone of inhibition

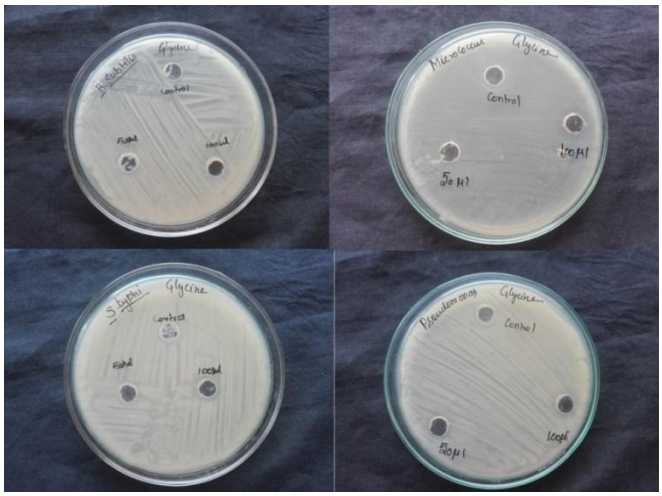

Figure 10a: Photographic view showing inhibition region of four different micro-organisms at 50µg/ml and 100 µg/l concentrations against glycine crystal

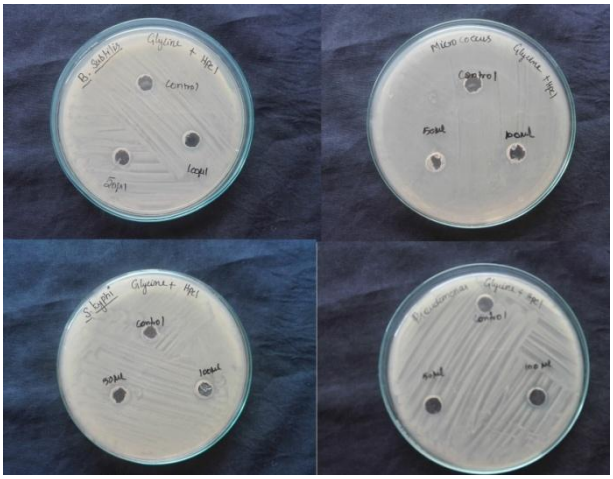

Figure 10b: Photographic view showing inhibition region of four different micro-organisms at 50µg/ml and 100 µg/l concentrations against glycinium dihydrogen complex crystal

From the Table 4, it is clear that glycine and its complex crystals have no antimicrobial activity against four different test bacteria. But, the glycine crystal shows the effective zone of inhibition (4 mm) for Micrococcus organism in 100 µl concentration**.**

5. Conclusion

The slow evaporation technique was used to grow the glycinium dihydrogen phosphate complex crystal successfully at room temperature. It has monoclinic crystal system with the space group $P2_1/c$ which was confirmed by single-crystal XRD technique. The average crystalline size of grown crystal was found to be as 27 nm from the PXRD patterns and the peaks were indexed using the INDX software. Further, the presence of various functional groups and elements were verified using FT-IR and FT-Raman spectroscopy and Energy dispersive X-ray studies. The SEM analyzes shows that the title crystal has smooth surface and well defined hexagonal shape. Also, the optical band gap was determined as 5.38 eV by UV- Visible spectroscopy technique. The grown parent and its complex crystals were involved in an antibacterial activity against certain four micro-organisms by disc diffusion method. This study revealed that the pure glycine and glycinium dihydrogen complex crystals have no bacterial screening effect.

Acknowledgement

The authors sincerely acknowledge their thanks to the Management and Principal of Devanga Arts College, Aruppukottai for their permission and encouragement during their research work.

References

1. Meerza Abdul Razak, Pathan Shajahan Begum, BuddollaViswanath, & Senthilkumar Rajagopal. (2017). Multifarious Beneficial Effect of Nonessential Amino Acid, Glycine: A Review, *Oxidative Medicine and Cellular Longevity*.2017, 1-8.
2. Sekhar, R.V., McKay, S.V., Patel, S.G., Guthikonda, A.P., Reddy, V.T., Balasubramanyam, A., & Jahoor, F. (2011). Glutathione synthesis is diminished in patients with uncontrolled diabetes and restored by dietary supplementation with cysteine and glycine. *Diabetes Care.Internet.*, 34(1), 162-167.
3. Valko, M., Leibfritz, & D., Moncol, J. (2007). Free radicals and antioxidants in normal physiological functions and human disease. *International Journal of Biochemistry & Cell Biology.* 39(1), 44-84.
4. Bouayed, J., & Bohn, T. (2010). Exogenous antioxidants—double-edged swords in cellular redoc state: health beneficial effects at physiologic doses versus deleterious effects at high doses. *Oxidative Medicine and Cellular Longevity*, 3(4), 228-237.
5. Davis, C.D., Tsuji, P.A., & Milner, J.A. (2012). Selenoproteins and Cancer Prevention. *Annual Review of Nutrition,* 32, 73-95.
6. Marsh, R.E. 1958. A Refinement of the Crystal Structure of Glycine. *Acta Crystallogr;* 11, 654 -663.
7. Iitaka, Y. (1960). The Crystal Structure of *β*-Glycine. *ActaCrystallogr.*, 13, 35-45.
8. Iitaka, Y. (1958). The crystal structure of γ-glycine. *ActaCrystallogr.*, 11, 225-226.
9. Dillip, G.R., Raghavaiah, P., Mallikarjuna, K., Madhukarreddy, C., Bhagavannarayana, G., Rameshkumar, V., & Devaprasadraju, B. (2011). Crystal growth and characterization of γ-glycine grown from potassium fluoride for photonic applications. *Spectrochim. Acta A*, 79, 1123-1127.
10. Fleck, M., Ghazaryan, V.V., & Petrosyan, A.M. (2010). Glycine hydrogen fluoride: remarkable hydrogen bonding in the dimeric glycine glycinium cation. *J. Mol. Struct*., 984, 83–88.
11. Sampath Krishnan, S., Balamurugan, N., Kumutha, R., Vidhyalakshmi, Y., & Muthu, R. (2012). Growth and characterisation of new nonlinear optical bis-glycinehydro bromide single crystal. *J. Min. Mater. Charact. Eng.*, 11, 597–607.
12. Sekar, C., & Parimaladevi, R. (2009). Effect of silver nitrate on the growth, optical, spectral, thermal and mechanical properties of γ-glycine single crystal. *J.Optoelect. Biomed. Mater*., 1, 215–225.

13. Ambujam, K. & Sagayaraj, P. (2006). Growth and characterization of a novel NLO crystal Bis glycine hydrogen chloride, *J. Cryst.Growth*, 286, 440–444.
14. Narayana Moolya, B., & Dharmaprakash, S.M. (2007). Synthesis, growth and characterization of a new semi organic nonlinear optical diglycine hydro bromide crystal, *Mater. Lett*., 61,3559–3562.
15. Uma devi, T., Lawrence, N., Ramesh Babu, R., Ramamurthi, K., & Bhagvan-narayanan, G. (2009). Structural, electrical and optical characterization studies on glycine picrate single crystal: a third order nonlinear optical material. *J. Min. Mater. Charact. Eng.*, 8, 755–763.
16. M.T. Averbuch-Pouchot, A. Durif, J.C. Guitel, Structures of glcine monophosphate and glycine cyclo-triphosphate. Acta Crystallogr. C44 (1988) 99–102.
17. Anitha, R., Athimoolam, S., Gunasekaran, M., & Anitha, K. (2014). X-ray, vibrational spectra and quantum chemical studies on a new semiorganic crystal: 4-Chloroanilinium perchlorate. *Journal of Molecular Structure*, 1076, 115–125.
18. Krishnakumar, V., & John Xavier, R. (2005). Density functional theory calculations and vibrational spectra of 3, 5-dibromopyridine and 3, 5- dichloro-2, 4, 6-trifluoropyridine, *Spectrochim. Acta A*, 61, 253–260.
19. Rajkumar, J. M., & Ramakrishnan, V. (2001). Vibrational spectroscopic study of DL-methionine dihydrogen phosphate. *Spectrochim. Acta A*, 57, 247-254.
20. Ravikumar, B., Rajaram, R.K., & Ramakrishnan, V. (2006). Raman and IR spectral studies of L-phenylalanine L-phenylalaninium dihydrogenphosphate and DL-phenylalaninium dihydrogenphosphate. *J. Raman Spectrosc*., 37, 597-605.
21. Chandran Muthuselvi, Arulanandam ShagayaPrincy and Sankara Sabapathy Pandiarajan. (2017). Growth and Characterization of 4-carboxyanilinium DihydrogenPhosphate Semi-organic Complex Crystal, Asian Journal of Applied Sciences, 10, 159-169.
22. Koleva, V. ,Stefovb, V., Najdoski, M., & Cahil, A. (2012). Vibrational spectra of cobalt dihydrogen phosphate dihydrate, Co (H_2PO_4) 2· $2H_2O$ *Vibrational Spectroscopy*, 62, 229-237.
23. Roseline Sebastian, Sr. S. H., Abdul-Malek, S., Al-Tamimi, Nasser, R., El-Brollosy, Ali A. El- Emam, Yohannan Panicker, C., & Christian Van Alsenoy. (2015).Vibrational spectroscopic (FT-IR and FT-Raman) studies, HOMO–LUMO, NBO analysis and MEP of 6-methyl-1-({[(2E)- 2-methyl-3-phenyl-prop-2-en-1-yl]oxy}methyl)-1,2,3,4-tetra hydroquinazoline-2,4-dione, a potential chemotherapeutic agent, using density functional methods, *Spectrochimica Acta Part A: Molecular and Biomolecular Spectroscopy,* 134: 316-325.
24. Panicker, C.Y., Varghese, H.T., Ambujakshan, K.R., Mathew, S., Ganguli, S., Nanda, A.K., Van Alsenoy, C., & Mary,Y.S. (2010).Vibrational spectra and computational study of 3-amino-2-phenyl quinazolin-4(3*H*)-one, *Journal of Molecular Structure,* 963, 137-144.
25. Yusuf Sert , S., Sreenivasa, Hatice Dogan, Mohan, N.R., Suchetan, P.A., & Fatih Ucun. (2014). Vibrational frequency analysis, FT-IR and Laser-Raman spectra, DFT studies on ethyl (2E)-2-cyano-3-(4-methoxyphenyl)- acrylate, *Spectrochimica Acta Part A: Molecular and Bio Molecular Spectroscopy,* 130, 96-104.
26. Muthuselvi, C., Pandiarajan, S., Ravikumar, B., Athimoolam, S., & R. Krishnakumar, R. V. (2018). Halogen Substituted Indeno Quinoxaline Derivative Crystal: A Spectroscopic Approach. *Asian Journal of applied sciences*, 11, 29-37.
27. Chinna Babu, P., Sundaraganesan, N., Sudha, S., Aroulmoji, V., & Murano, E. (2012). Molecular structure and vibrational spectra of Irinotecan: A density functional theoretical study, *Spectrochimica Acta Part A: Molecular and Biomolecular Spectroscopy,* 98, 1-6.
28. Muthuselvi, C., Pandiarajan, S., & Krishnakumar, R.V. (2016). Vapor Diffusion Growth and Characterization of Aspirin–Perchloric acid Complex Crystal. *Elixir Vib. Spec.*, 2016, 95, 40673-40678.
29. Muthuselvi, C., Dhavachitra, M., & Pandiarajan, S. (2016). Growth and Characterization of Aspirin Crystal in the Phosphoric acid Medium. *Journal of Chemical and Pharmaceutical Research*, 8(5), 804-814.

30. Baran, E.J., Viera, I., & Torre, M.H. (2007) Vibrational spectra of the Cu(II) complex of L-asparagine and Lglutamine. *Spectrochim.Acta*. 66A, 114-117.